Mutation of an essential glutamate residue in folylpolyglutamate synthetase and activation of the enzyme by pteroate binding

ARTICLE *in* ARCHIVES OF BIOCHEMISTRY AND BIOPHYSICS · JULY 2002

Impact Factor: 3.02 · DOI: 10.1016/S0003-9861(02)00040-1 · Source: PubMed

ACADEMIC PRESS

Archives of Biochemistry and Biophysics 402 (2002) 94–103

ABB

www.academicpress.com

Mutation of an essential glutamate residue in folylpolyglutamate synthetase and activation of the enzyme by pteroate binding

Yi Sheng,[a] Jennifer A. Cross,[c] Yang Shen,[b] Clyde A. Smith,[c] and Andrew L. Bognar[a,b,*]

[a] *Department of Laboratory Medicine and Pathobiology, University of Toronto, 1 King's College Circle, Toronto, Ont., Canada M5S 1A8*
[b] *Department of Medical Genetics and Microbiology, University of Toronto, 1 King's College Circle, Toronto, Ont., Canada M5S 1A8*
[c] *School of Biological Sciences, University of Auckland, Auckland, New Zealand*

Received 20 December 2001, and in revised form 19 February 2002

Abstract

Site-directed mutagenesis was performed on Glu143, an essential amino acid in *Lactobacillus casei* folylpolyglutamate synthetase (FPGS) and the structurally equivalent residue, Glu146, in *Escherichia coli* FPGS. Glu143 is positioned near the P-loop and interacts with the Mg^{2+} of Mg NTP-binding proteins. We have solved the structure of the E143A mutant of *L. casei* FPGS in the presence of AMPPCP and Mg^{2+}. The structure showed a water molecule at the place where Mg^{2+} bound to the wild type enzyme. Mutant proteins E143A, and even E143D and E143Q with conservative mutations, lacked enzyme activity and failed to complement the methionine auxotrophy of the *E. coli folC* mutant SF4, showing that Glu143 is an essential residue. Both the *L. casei* and the *E. coli* FPGS mutant proteins bound methylene-tetrahydrofolate diglutamate and dihydropteroate normally. The *E. coli* E146Q mutant FPGS bound ADP with the same affinity as the wild type enzyme but bound ATP with much lower affinity and had higher ATPase activity than the wild type enzyme. The mutant enzyme was defective in forming the acyl-phosphate reaction intermediate from ATP and dihydropteroate. The *E. coli* FPGS requires activation by dihydropteroate or tetrahydrofolate binding to allow full activity. In the absence of a pteroate substrate, only 30% of the total enzyme binds ATP. We suggest that dihydropteroate causes a conformational change to allow increased ATP binding. The mutant enzyme was similarly activated by dihydropteroate resulting in increased ADP binding.

Keywords: Folylpolyglutamate synthetase; Mutagenesis; Mg binding; ATP binding; Enzyme activation by pteroates

Folate coenzymes exist in cells primarily as poly-γ-glutamate derivatives. Folate polyglutamates are often more effective substrates and regulators of folate-dependent enzymes [1,2]. Polyglutamates are preferentially retained in *Lactobacillus casei* and in mammalian cells. Polyglutamylation of antifolates that contain glutamate is important to their pharmacological efficacy [3–5]. Folylpolyglutamate synthetase (FPGS)[1] (EC 6.3.2.17) catalyzes the MgATP-dependent ligation of L-glutamate to tetrahydrofolate coenzymes or to antifolates at the γ-carboxyl of the terminal glutamate to form polyglutamate derivatives. The *Escherichia coli* FPGS also catalyzes the ligation of glutamate to dihydropteroate to form dihydrofolate with an activity referred to as dihydrofolate synthetase (DHFS) activity. Organisms that biosynthesize folates de novo possess DHFS activity. In bacteria DHFS is usually associated with FPGS activity [6] but DHFS is a separate enzyme in yeast.

FPGS is a promising target enzyme for antimicrobial and anticancer chemotherapy because it is essential for folate biosynthesis in organisms that make folate and for folate and antifolate retention in those that do not. Understanding the structure and mechanism of FPGS is important for the design of compounds that act as inhibitors or as substrates that require polyglutamylation to be effective inhibitors of other folate-dependent enzymes.

* Corresponding author. Fax: +416-978-6885.
E-mail address: a.bognar@utoronto.ca (A.L. Bognar).

[1] *Abbreviations used:* FPGS, folylpoly-γ-glutamate synthetase; MurD, UDP-*N*-acetylmuramoyl-L-alanine:D-glutamate ligase; DHFS, dihydrofolate synthetase; $H_4PteGlu_2$, tetrahydrofolate diglutamate; AMPPCP, β,γ-methylene adenosine triphosphate; ACP4, β,γ-methylene adenosine tetraphosphate; rms, root mean square; THF, tetrahydrofolate; DMSO, dimethyl sulfoxide; K_d, dissociate constant.

0003-9861/02/$ - see front matter
PII: S0003-9861(02)00040-1

We are interested in the active site residues involved in the mechanism of catalysis of FPGS. Recently the three-dimensional structure of the FPGS from *L. casei* was solved by X-ray crystallography [7]. The enzyme consists of two domains connected by a single loop. The active site is in the cleft between the two domains. The amino terminal domain of FPGS has the same fold as found in a broad group of mononucleotide-binding proteins [8]. The closest structural homolog to FPGS is MurD, UDP-*N*-acetylmuramoyl-L-alanine: D-glutamate ligase, an enzyme essential for peptidoglycan synthesis [9,10].

Adjacent to the P-loop in the *L. casei* FPGS active site is Glu143, which coordinates with the magnesium ion of Mg^{2+} ATP [7], suggesting that this residue is involved in the catalytic mechanism of the enzyme. Recently, the crystal structures of FPGS · MgAMPPCP complexes and FPGS · MgACP4 · methylene-THF were solved [11]. These structures show a difference in the conformation of FPGS between the binary and ternary complexes. Analysis of these structures led us to predict that folate binding is required for the adenine of ATP to bind specifically and that the conformational change associated with folate binding creates the site to which the glutamate substrate binds [11].

In this study we describe the mutagenesis of Glu143 in the *L. casei* FPGS and the corresponding residue Glu146 in the FPGS from *E. coli* and the effect of the mutations on enzyme activity and substrate binding. We also show that the binding of ATP and ADP to wild type *E. coli* FPGS is enhanced in the presence of dihydropteroate or tetrahydrofolate substrates.

Materials and methods

Reagents. (6*RS*)-5,6,7,8-Tetrahydrofolate and pteroic acid were from Schircks Laboratories, Switzerland. 5,10-Methylene-tetrahydrofolate was prepared from tetrahydrofolate by addition of formaldehyde in excess to the assay mix. 7,8-Dihydropteroate was prepared by reduction of pteroic acid with sodium dithionite and stored at −70 °C. [^{3}H]H_4PteGlu$_2$ was prepared from tetrahydrofolate using *E. coli* FPGS with the assay conditions described below, followed by purification on DEAE-cellulose (DE52) and Biogel P2 columns.

PCR-based site-directed mutagenesis. Oligonucleotide primers used for site-directed mutagenesis are as follows: *L. casei* FPGS E143A, 5′-AATTGCTCTTCC CTG AAT CAC CGC AAC ATC AAC CTG ACG-3′, 5′-AATTGCTCTTCC CAG GTC GGT ATT GGC GGC GAC ACG G-3′; E143D, 5′-AATTGCTCTTCC ATC AAT CAC CGC AAC ATC AAC CTG ACG-3′, 5′-AATTGCTCTTCC GAT GTC GGT ATT GGC GGC GAC ACG G-3′; E143Q, 5′-AATTGCTCTTCC TTG AAT CAC CGC AAC ATC AAC CTG ACG-3′, 5′-AATTGCTCTTCC CAA GTC GGT ATT GGC GGC GAC ACG G-3′; *E. coli* FPGS E146Q, 5′-AATTGCTCTTCC CAA GTA GGG CTG GGC GGT CGT CTG GAC G-3′, 5′-AATTGCTCTTCC TTG CAG AAT CAC CAC GTC AAG TTG TGC C-3′; Stop codon for complementation, 5′-GGG GAA AAT CAT GAT TTG CCA AGG GAA CCA ATG TTT TAA TGG-3′.

Mutagenesis was performed on the *L. casei* FPGS or *E. coli* FPGS genes directly in the expression plasmid pCYB1 (NEB). Mutations were introduced using pairs of oligonucleotide primers containing a *Sap*1 site at their 5′ ends. *Sap*1 cuts these sites leaving 5′ cohesive ends between 1 and 4 bp downstream of the target sequence. The desired mutation(s) were placed within the three nucleotides of the cohesive ends and complemented by the corresponding sequence encoded by the second primer. PCR (30 cycles) was used to generate the entire recombinant plasmid outward from the mutagenized sequence as a linear DNA fragment with a *Sap*1 site at both ends using Expand-long PCR polymerase (BMH). The DNA fragment was digested with *Sap*1 and ligated with T4 ligase. The template plasmid was removed by digestion with *Dpn*1. Candidate mutant genes were sequenced to verify that only the desired mutations were present.

Expression and purification of FPGS mutants. Each plasmid encoding a mutant protein was transformed into *E. coli* strain BL21 for expression. FPGS mutants were expressed as fusion proteins using the IMPACT system from NEB. The cultures were induced with 1 mM IPTG at 30 °C for 6 h. The crude extracts were loaded on a chitin column and the fusion proteins were cleaved with 50 mM DTT in 10 mM Tris–HCl, pH 7.5, 1 M NaCl for 24 h at room temperature. The eluted proteins were dialyzed against 10 mM Tris–HCl, pH 7.5, 200 mM KCl, and stored at −70 °C with 20% Me_2SO (samples used for CD study were stored with 50% glycerol instead of 20% Me_2SO). Protein concentration was determined by the Bradford assay (Bio-Rad).

Complementation studies. The *E. coli* SF4 strain was grown in Vogel–Bonner minimal medium [12] supplemented with methionine (50 μg/ml) and glycine (50 μg/ml). Minimal medium lacking methionine or glycine was used in complementation analysis. A "TAA" translation stop codon (see above) was inserted at the end of each mutant FPGS gene with the Transformer Site-Directed Mutagenesis method (Clontech Laboratories) [13], such that the native FPGS mutant proteins, rather than the fusion proteins, would be expressed. These mutant genes were transformed into the SF4 strain and grown in LB medium supplemented with ampicillin (50 μg/ml). Transformants were replica plated onto minimal plates to determine whether the mutant genes complemented the methionine auxotrophy.

FPGS enzyme activity assay. Enzyme activities were measured by the incorporation of [^{3}H]glutamate into 5,10-methylene-tetrahydrofolate, tetrahydrofolate or dihydropteroate as described by Shane [14]. A standard *L. casei* FPGS assay mix consisted of 100 mM Tris, 50 mM Glycine, pH 9.75, 200 mM KCl, 10 mM $MgCl_2$, 5 mM DTT, 10% DMSO, 5 mM ATP, 250 μM L-glutamate, 1.25 μCi [^{3}H]glutamate, 100 μM tetrahydrofolate, 12 mM formaldehyde, and 5–10 μg pure enzyme. For the *E. coli* FPGS assay, either tetrahydrofolate (no formaldehyde added) or dihydropteroate was used as substrate, rather than 5,10-methylene-tetrahydrofolate.

Spectroscopic measurement. CD measurements were conducted on an AVIV 62DS spectrometer. Near UV CD spectra were recorded in a 1.0 cm quartz cell in a buffer containing 10 mM Tris–HCl, pH 7.5, 250 mM KCl, 1 mM EDTA, and 1% glycerol at room temperature.

Equilibrium dialysis. Microdialysis cells with dialysis membrane (MW cutoff 12 kDa) were used. One chamber was filled with 120 μl FPGS protein (1.5 mg/ml) in 10 mM Tris–HCl, pH 7.5, 200 mM KCl, 10 mM $MgCl_2$, and 10% DMSO (P-side). The other side was filled with various concentrations of [γ-^{32}P]ATP, [α-^{32}P]ATP, 8-[^{14}C]ADP or [^{3}H]tetrahydrofolate diglutamate in 120 μl of the same buffer as the P-side. The equilibrium was allowed to proceed for 48 h at 4 °C and the amount of labeled substrate in both sides was measured. Equilibrium dialysis experiments were repeated at least twice for each substrate. Each figure shows representative data from at least two independent experiments. Each point in the plot represents the mean of three determinations from one representative experiment. Bound substrates were calculated according to the following formula:

$$\frac{\mathrm{CPM}_{\text{protein side}} - \mathrm{CPM}_{\text{ligand side}}}{\text{Total CPM}} \times \text{Total substrate (mole)}.$$

Data are presented as ratio of bound substrate (mole)/Total FPGS (mole).

Determination of dihydropteroate binding to E. coli FPGS by fluorescence titration. The binding constants for dihydropteroate of the wild type and E146Q mutant FPGS enzymes of *E. coli* were determined by the increased fluorescence of dihydropteroate when bound to the enzyme. Fluorescence was measured at different concentrations of dihydropteroate (0–100 μM) using a Photon Technology International QM-1 fluorescence spectrophotometer equipped with excitation intensity correction. Each 0.5 ml sample contained 50 μg protein in 10 mM Tris–HCl (pH 7.5), 200 mM KCl, and 10 mM $MgCl_2$. Samples were excited at 317 nm and emission was at 400 nm with the excitation and emission bandpass set at 4 nm. The K_d's were determined by fitting the fluorescence data to a hyperbolic regression analysis program HYPER (version 1.0)

TLC analysis of nucleotides bound to FPGS after equilibrium dialysis. Equilibrium dialysis was done with *E. coli* FPGS incubated with [α-^{32}P]ATP and the sample from the chamber containing the protein was applied to a Sephadex G50 spin column. The void volume was chromatographed on a PEI-cellulose TLC plate (Caledon Labs) with a liquid phase of 0.75 M KH_2PO_4, pH 3.5 to identify nucleotides bound to the enzyme. The total nucleotides in the chambers containing both protein and ligand and ligand alone were determined by chromatography on TLC without prior gel filtration.

Assay for the acyl-phosphate intermediate. A reaction mix (15 μl) containing 30 μg FPGS, 100 μM ATP, 10 μCi [γ-^{32}P]ATP in 10 mM Tris–HCl, pH 7.5, 200 mM KCl, 10 mM $MgCl_2$, 10% DMSO, 1 mM DTT, with 200 μM dihydropteroate was incubated at 37 °C for 90 min. The reaction was stopped with 5 μl of cold 10 mM ATP, 10 mM ADP, 0.3 mM EDTA, pH 8.0, and boiled for 5 min to denature the enzyme. The mixture was chromatographed on a PEI-cellulose TLC plate (Caledon Labs) with a liquid phase of 1 M formate, 0.5 M LiCl, dried and autoradiographed. As a positive control for phosphate release, 2 mM L-glutamate was added to the reaction mixture to allow turnover of the enzyme.

X-ray crystal structure determination. Crystals of the E143A mutant of *L. casei* FPGS were grown by microseeding from 50 to 100 mM CAPSO buffer, pH 9.5, and 16–26% PEG4000. Prior to crystallization, the protein at a concentration of 10 mg/ml was incubated overnight at 4 °C with 5 mM AMPPCP and 10 mM $MgCl_2$. The protein (2 μl) was then mixed with CAPSO/PEG4000 solutions (4 μl) to give the final concentrations of buffer and PEG in the ranges given above, and left to incubate for 4–6 h. The samples were centrifuged to remove any precipitated protein, placed into microbridges, and seeded with microcrystals from preliminary hanging drop experiments. Crystals with typical dimensions $0.5 \times 0.2 \times 0.1$ mm generally grew over the course of 1–3 days at 18 °C.

The E143A crystals are essentially isomorphous with the wild type *L. casei* FPGS crystals [6], with cell dimensions $a = 53.3$ Å, $b = 45.5$ Å, $c = 84.2$ Å, and $\beta = 107.0°$ belonging to space group $P2_1$. X-ray diffraction data were collected from a single flash-frozen crystal at 100 K. The crystal was transferred into a solution containing 0.065 mM CAPSO (pH 9.5), 18% PEG4000, and 25% ethylene glycol just prior to freezing. The data were collected using a MAR345 imaging plate detector mounted on a Rigaku Ru-H3R rotating anode generator running at 50 kV and 100 mA. A total of 340 images were collected to a resolution of 2.4 Å and processed using the HKL suite of programs [15]. Relevant data collection statistics are given in Table 1.

Despite the closely isomorphous nature of the E143A crystals relative to the wild type MgATP · FPGS crystals (the maximum decrease in cell dimensions due to

Table 1
Data collection and refinement statistics

Data collection	
Maximum resolution (d_{min}) (Å)	2.4
Total observed reflections to d_{min}	191,012
Unique reflections to d_{min}	
Multiplicity	15.5
R_{merge}[a] (in high resolution shell[b]) (%)	13.5 (46.6)
Completeness (%)	98.4 (95.8)
Average I/σ	10.5 (2.2)
Refinement	
Resolution range (Å)	20.0–2.4
R_{work} (%)[c]	20.3
R_{free} (%)[d]	25.2
Reflections used (work/free) (%)	13,000/560
Total atoms	
Protein	3000
Solvent	150
rms Deviation from ideality	
Bonds (Å)	0.019
Angles (°)	1.78
Average *B*-value[e] (protein/solvent) (Å^2)	32.5/45.6

[a] $R_{merge} = \sum |I - \langle I \rangle| / \sum I \times 100$, where I is the observed intensity and $\langle I \rangle$ is the mean intensity.
[b] 2.5–2.4 Å.
[c] $R = \sum ||F_o| - k|F_c|| / \sum |F_o| \times 100$.
[d] Calculated with 5% of the reflections.
[e] Temperature factor.

freezing was just over 1%, with an overall decrease in unit cell volume of about 3%), the initial *R*-factor calculated between the MgATP · FPGS model and the E143A data was rather high at 49.7%. Although this was probably due to the cell shrinkage and a translation or rotation of the molecule in the unit cell, a change in the relative orientations of the N- and C-terminal domains due to the point mutation could not be discounted. Therefore molecular replacement with the program AMORE [16] was used to position the molecule within the cell. Two models were used, the whole MgATP · FPGS model (model 1) and the individual N- and C-terminal domains of MgATP · FPGS (model 2). In both cases the pyrophosphate anion, Mg^{2+} ion, and the solvent molecules were removed from MgATP · FPGS, and the side chain of Glu143 was truncated to alanine. Model 1 gave a correlation coefficient and *R*-factor of 0.65 and 34.5%, respectively, while the corresponding values using model 2 were 0.68 and 33.7%, indicative of no significant movement of the C-terminal domain relative to the N-terminal domain. The structure was subsequently refined with CNS [17] and some relevant refinement statistics are given in Table 1.

Results

Characterization of Glu143 mutants of L. casei FPGS. Glu143 of the *L. casei* FPGS was mutated to Ala, Asp, and Gln. FPGS was expressed in *E. coli* as a fusion protein with C-terminal intein and chitin-binding domains. The fusion protein was cleaved and purified as described in Materials and methods. This procedure yielded 1 mg pure enzyme per liter of culture and there was no apparent difference between the yield of the wild type and mutant enzymes (not shown). The CD spectrum of the mutant proteins was identical to the spectrum of native wild type enzyme and did not resemble that of enzyme denatured with guanidine HCl, suggesting that the mutations caused no gross changes in enzyme folding or structure (not shown). There was a background activity in enzyme assays using the purified mutant enzymes (Table 2) but the activity did not increase with enzyme or substrate concentration, suggesting that the mutant proteins were completely inactive. To assess mutant enzyme function in vivo, a translation stop codon was inserted into the mutant FPGS genes cloned in the expression plasmid to correctly terminate the translation of the FPGS gene products. The plasmids expressing the properly

Table 2
Relative activity[a] of *L. casei* FPGS and *E. coli* FPGS mutants and binding constants for 5,10-methylene-tetrahydrofolate diglutamate[b]

	Enzyme activity velocity (nmol/mg/h)	Relative activity (%)	SF4 complementation	K_d 5,10-methylene-tetrahydrofolate diglutamate (μM)
L. casei FPGS[c]				
Wild type	12,000	100	Yes	19 ± 3.9
E143A	20	0.17	No	22 ± 5.0
E143D	33	0.28	No	18 ± 1.3
E143Q	30	0.26	No	16 ± 4.6
E. coli FPGS[d]				
Wild type	12,500	100	Yes	
E146Q	ND[e]		No	

[a] FPGS activity was assayed and kinetic constants determined as described in Materials and methods.
[b] Equilibrium dialysis was performed as described in Materials and methods. The dialysis was done in the presence of 5 mM ATP.
[c] The *L. casei* FPGS activity was determined using 5,10-methylene-tetrahydrofolate as the substrate.
[d] The *E. coli* FPGS activity was determined using tetrahydrofolate as the substrate.
[e] Not detectable.

terminated FPGS mutant genes were used to transform the *E. coli folC* strain SF4 [18]. Whereas the wild type *L. casei* FPGS expressed in this construct could complement the methionine auxotrophy of strain SF4, no complementation was seen with the mutant enzymes (Table 2), confirming that the mutants had no activity.

Although the Glu143 mutants were inactive, we wanted to determine whether the enzyme could bind its substrates. Equilibrium dialysis studies (Table 2) showed that [^{3}H]H_4PteGlu$_2$, which is a good substrate for *L. casei* FPGS [19], could bind to the wild type and mutant enzymes with similar affinity ($K_d = 19 \pm 3$ μM). These results were obtained in the presence of 5 mM ATP but folate binding was essentially the same in the absence of ATP for both the wild type and mutant enzymes.

X-ray crystal structure of the E143A mutant enzyme. The refined E143A model consists of 3000 protein atoms (400 residues, 1–146, 151–169, 175–340, 346–377, and 382–425) and 150 solvent molecules (assumed to be water). The structure is essentially identical to the MgATP · FPGS structure [7]; the overall *rms* deviation in all Cα positions is 0.65 Å, while the individual domains show a similar degree of overlap (0.54 Å for the N-terminal domain and 0.62 Å for the C-terminal domain).

During the refinement and model rebuilding, special attention was paid to residue 143 and the region of the structure near the ATP binding P-loop (residues 46–50). Even from the first electron density maps it was clear that the side chain of residue 143 was missing. A water molecule has been modeled near the position formerly occupied by the carboxylate group, hydrogen bonded to the main chain amide nitrogen of residue Thr72 (Fig. 1). A second electron density peak was observed adjacent to the carbonyl oxygen of Ser73 approximately 1.0 Å from the position occupied by the essential Mg^{2+} in the MgATP · FPGS structure [6]. The spherical shape of the density and its distance from the carbonyl oxygen (2.9 Å) suggest that the position of the Mg^{2+} is occupied by a water molecule. When Mg^{2+} is modeled into this site, the temperature factor refines to 7.5 Å^2, significantly lower than the temperature factors of the surrounding atoms (an average of 28.5 Å^2), while the temperature factor of a water molecule is 29.2 Å^2. This is also consistent with a water molecule replacing the Mg^{2+} ion in the E143A mutant.

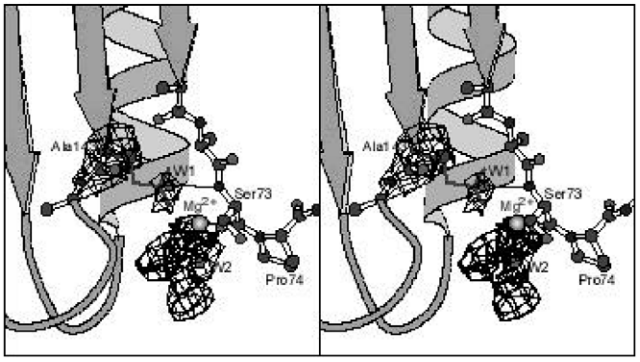

Fig. 1. Stereoview of the active site of the E143A mutant of *L. casei* FPGS. The electron density of Ala143 is shown, along with the densities of two water molecules (W1 and W2) which occupy the positions of the glutamate side chain (thick gray bonds) and the Mg^{2+} ion (gray sphere) in the wild type structure. The residual $F_o - F_c$ electron density is shown as dashed lines, and the position of the pyrophosphate ion in the wild type structure is indicated (thick black bonds).

To address the question of whether AMPPCP is bound to the mutant, an $F_o - F_c$ difference electron density map was calculated at the end of refinement. There were three large peaks adjacent to the P-loop, arranged in an L-shape (Fig. 1). When the MgATP · FPGS complex is superimposed on the E143A structure based upon the secondary structure elements in the N-terminal domain, two of the peaks coincide with the two phosphate groups of the pyrophosphate. When a similar superposition is performed with a ternary AMPPCP · methylene-THF · FPGS complex [19], the α- and β-phosphate groups of the AMPPCP overlap the same two electron density peaks, with the γ-phosphate group positioned near the water molecule which interacts with Ser73. The density can be modeled as either (i) a single pyrophosphate molecule in an orientation similar to that observed in the MgATP · FPGS structure, (ii) two pyrophosphate molecules in two different orientations with one phosphate in common, or (iii) a triphosphate moiety. In the first case, a water molecule would occupy the third peak, while in the third, the triphosphate would have to almost double back on itself in a rather strained L-shaped conformation. The second case implies some degree of disorder in the nucleotide molecule, and given that we see no electron density for the ribose or adenine moiety, this might be the most plausible explanation. These results suggest that if ADP is bound, the α- and β-phosphates partially occupy a location as would be expected for ATP, yet with the ribose and adenine groups are not firmly anchored to the protein. If on the other hand AMPPCP is bound at the active site then the triphosphate moiety appears to be bound in a non-specific, non-productive conformation.

The only other observed difference is in the position of the conserved Lys50 side chain. This residue is part of the P-loop consensus sequence, and plays an important role in ATP-binding and possibly hydrolysis. In the wild type structure, the Nζ atom is hydrogen bonded to an oxygen atom on the pyrophosphate moiety at a distance of 2.4 Å. In the E143A mutant, the equivalent distance would be between 3.6 and 3.8 Å, which suggests that either AMPPCP is not bound in the active site, or it is bound such that it no longer makes specific interactions with the P-loop.

Characterization of the wild type and E146Q mutants of E. coli FPGS. Since glutamate 143 is in the MgATP binding pocket and is required for magnesium binding,

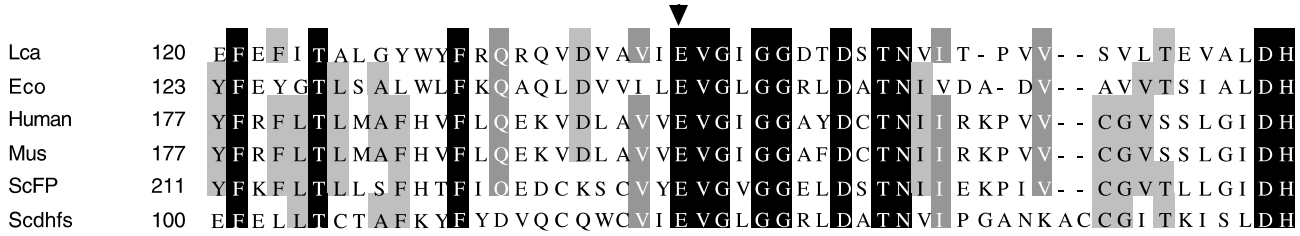

Fig. 2. Amino acid sequence alignment of FPGS genes from prokaryotic and eukaryotic species. The position of glutamate 143 of *L. casei* FPGS aligned with *E. coli* glutamate 146 is indicated by the arrow.

we wished to determine whether the mutation affects ATP binding. Equilibrium dialysis studies of ATP binding could not be done with the *L. casei* FPGS because the high K_m (3 mM) made it impossible to have high enough protein concentrations to sequester the substrate. However, the *E. coli* folylpolyglutamate synthetase–dihydrofolate synthetase (FPGS–DHFS) has an apparent K_m for ATP of 70 μM for the FPGS activity and 7 μM for the DHFS activity, respectively [20]. The higher affinity for ATP made equilibrium dialysis studies of ATP binding possible using this enzyme and we used the DHFS activity in our studies. Glu146 of the *E. coli* FPGS occupies the same position in the sequence alignment of the enzyme as Glu143 does in the *L. casei* FPGS (Fig. 2). An E146Q mutant was constructed in the *E. coli* enzyme, expressed, and purified using the same procedures as for the *L. casei* FPGS mutants. The E146Q mutant had no detectable enzyme activity but bound dihydropteroate with an apparent K_d of 10 μM, similar to the wild type enzyme (Fig. 3).

ATP binding to the wild type and E146Q mutant FPGS and its enhancement by dihydropteroate. Equilibrium dialysis studies with the *E. coli* FPGS using [γ-^{32}P]ATP showed binding of ATP to the free wild type enzyme, with a K_d of 76 μM (Fig. 4a). In contrast, no ATP binding was observed with the E146Q enzyme within the sensitivity of our assay. However, when [α-^{32}P]ATP was used, equilibrium dialysis studies showed that both the wild type and mutant enzymes bound ATP with the same affinity (Fig. 4b). The difference in binding between [α-^{32}P]ATP and [γ-^{32}P]ATP suggested that the [α-^{32}P]ATP binding observed was really binding to ADP or AMP produced by chemical hydrolysis or ATPase activity. In support of this hypothesis, Fig. 4c shows that ADP binding by the E146Q mutant enzyme was identical to the wild type enzyme and similar to its [α-^{32}P]ATP binding. Both ATP and ADP bindings saturated at 10–40% of the total enzyme being bound when the experiment was done in the absence of dihydropteroate.

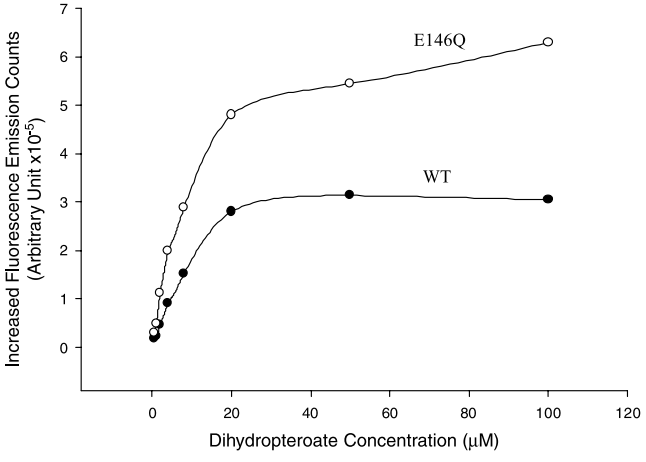

Fig. 3. Binding of dihydropteroate to *E. coli* FPGS wild type (•) and the E146Q mutant (○) measured by increased fluorescence at 400 nm. The binding was done in the presence of 5 mM ATP.

The enhancement of ATP binding in the presence of dihydropteroate (Figs. 4 and 5) or, to a lesser extent, tetrahydrofolate (Fig. 5) was seen as an increase in the proportion of the wild type enzyme bound by ATP. Nearly 100% of the protein was bound to ATP in the presence of dihydropteroate, suggesting that dihydropteroate binding activated FPGS (Fig. 4a). This suggests that dihydropteroate binding caused a conformational change in the inactive fraction of the FPGS, which allowed it to bind ATP. The optimal concentration of dihydropteroate or tetrahydrofolate for this effect was 10 μM. At higher concentrations, tetrahydrofolate significantly inhibited ATP binding with 60% inhibition at 100 μM THF, while dihydropteroate only inhibited binding by 5% at that concentration (Fig. 5). The binding of [α-^{32}P]ATP and ADP to the E146Q FPGS mutant was enhanced by dihydropteroate in the same manner as the wild type enzyme (Figs. 4b and c), suggesting that the mutant also undergoes the conformational change resulting in enzyme activation.

ATPase activity of wild type and E146Q mutants of E. coli FPGS. The equilibrium dialysis reaction mixture was passed through a Sephadex G50 spin-column and the enzyme-bound fraction in the void volume was chromatographed on TLC as described in Materials and methods. Fig. 6a shows that all the nucleotides bound to the mutant protein comigrated with ADP (lane 2), while the wild type enzyme bound mostly ATP and some ADP (lane 1). These results verify that the mutant FPGS binds ADP but very little ATP. Fig. 6b shows the TLC analysis of the equilibrium dialysis mixture without it

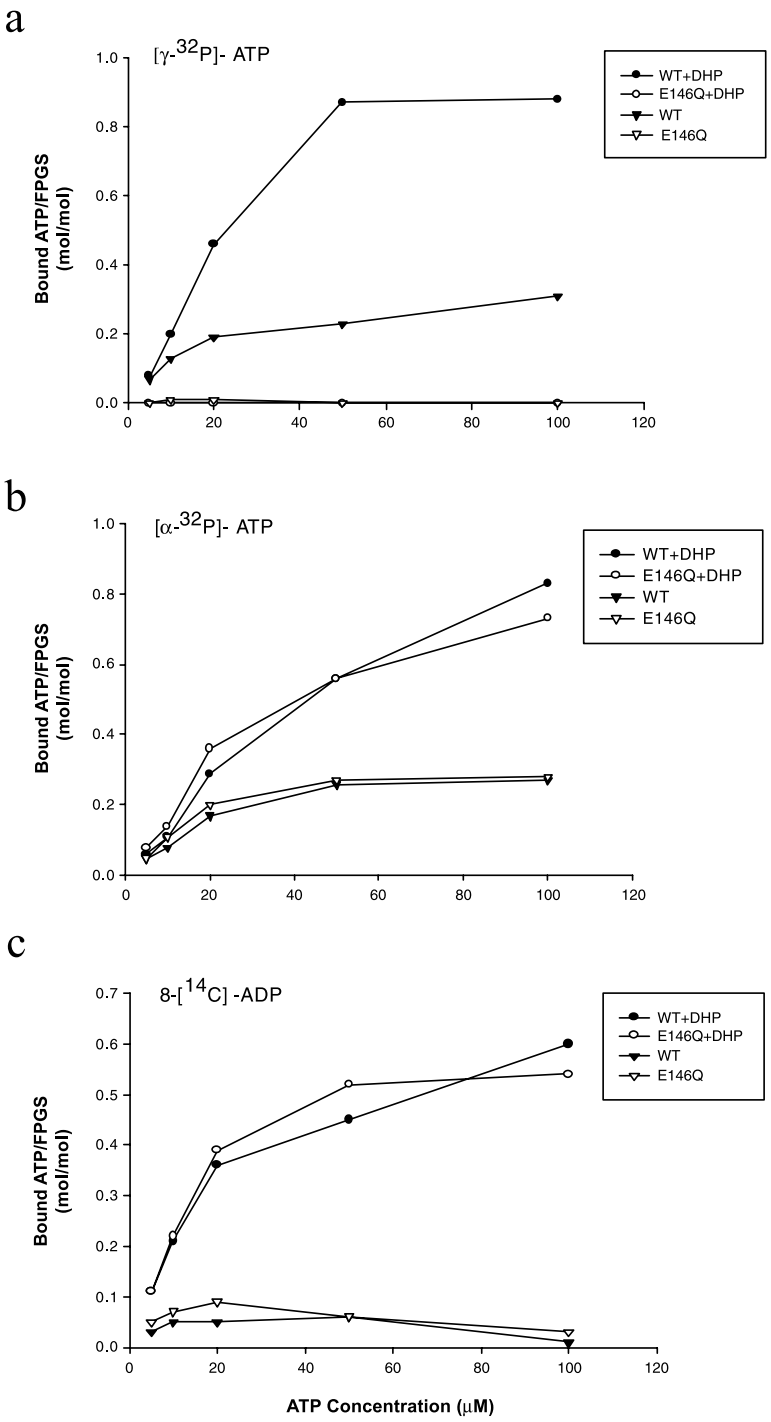

Fig. 4. Binding of [γ-^{32}P]ATP, [α-^{32}P]ATP or 8-[^{14}C]ADP to *E. coli* FPGS wild type and the E146Q mutant and effect of dihydropteroate on ATP binding. *E. coli* FPGS wild type (●, ▼) and mutant E146Q (◯, ▽) (30 μM) were subjected to equilibrium dialysis against the indicated concentration of free [γ-^{32}P]ATP (a), [α-^{32}P]ATP (b), or 8-[^{14}C]ADP (c) in the dialysis buffer (120 μl per chamber) containing 10 mM Tris (pH 7.5), 200 mM KCl, 10 mM $MgCl_2$ and 10% DMSO in the absence (triangles) or presence (circles) of 200 μM dihydropteroate.

being passed through Sephadex G50. There was no ADP in the BSA control (lanes 3 and 6) showing that ADP production was not due to chemical breakdown of the ATP but due to ATPase activity of FPGS. The ADP content of the compartment containing the mutant FPGS (lanes 4 and 5) is greater than that of the compartment containing the wild type enzyme (lanes 1 and 2), suggesting that the ATPase activity of the mutant is higher than the wild type enzyme. More than 50% of the ATP in the compartment has been converted to ADP by the mutant enzyme, suggesting that ADP production is not the result of a low level contaminant that copurifies

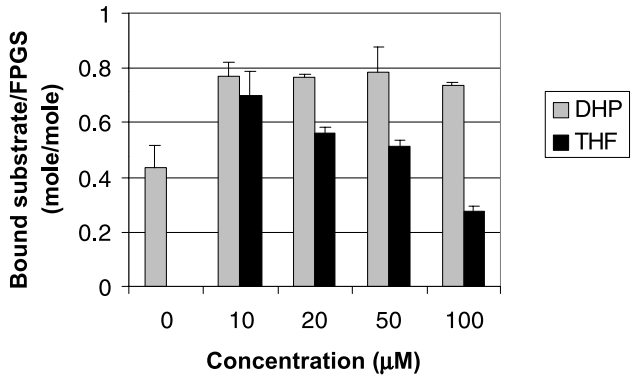

Fig. 5. Effect of dihydropteroate and tetrahydrofolate on *E. coli* FPGS ATP binding. Equilibrium dialysis was performed on wild type *E. coli* FPGS in the presence of the indicated concentration of dihydropteroate (gray bar) or tetrahydrofolate (black bar) and bound ATP/FPGS (mol/mol) is shown. The values are the means of three determinations from a single dialysis experiment, except for the value with no added dihydropteroate or tetrahydrofolate, which is the mean of two separate experiments done under the same conditions on the same day.

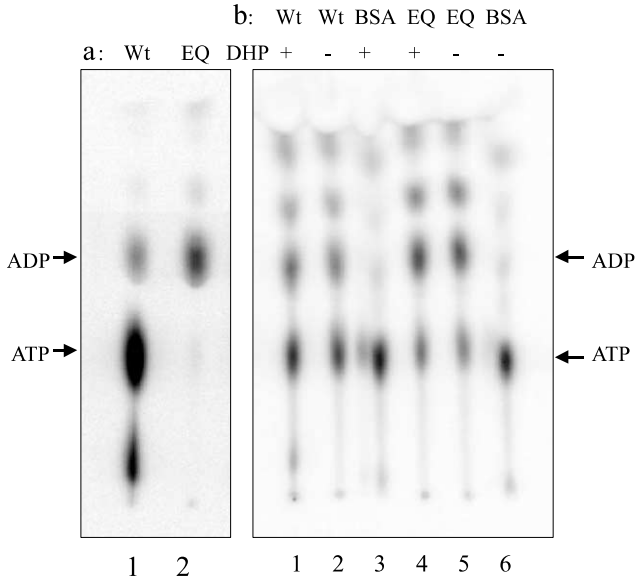

Fig. 6. (a) TLC analysis of nucleotides bound to FPGS after equilibrium dialysis. Equilibrium dialysis was performed in the presence of 100 μm [α-^{32}P]ATP as described in Materials and methods. 100 μl from the chamber containing the protein was applied to a Sephadex G50 spin column. The sample from the void volume was applied to a TLC plate and chromatographed as described in Materials and methods. Lane 1, wild type FPGS; lane 2 E146Q mutant FPGS. (b) TLC analysis of nucleotides present in equilibrium dialysis chambers. Lanes 1 and 2 contained wild type FPGS; lanes 4 and 5 contained mutant FPGS; lanes 3 and 6 contained BSA. Dihydropteroate (200 μM) was added to lanes 1, 3, and 4.

with FPGS. However, the TLC assays showed that ATP was not extensively degraded in the absence of enzyme during the equilibrium dialysis so the lack of ATP was not the cause of our inability to detect its binding to the mutant enzyme.

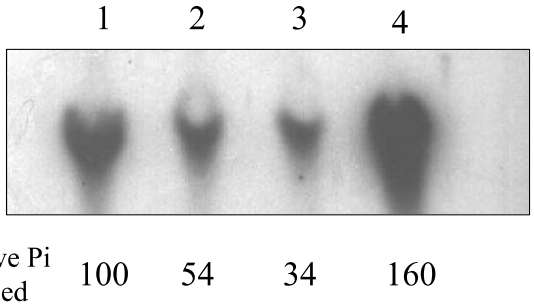

Fig. 7. TLC assay for formation of the acyl-phosphate reaction intermediate by wild type and E146Q mutant *E. coli* FPGS. Wild type *E. coli* FPGS and the E146Q mutant were incubated with 100 μM [γ-^{32}P]ATP and 200 μM dihydropteroate for 90 min, boiled for 5 min, and chromatographed on TLC as described in Materials and methods. 2 mM L-glutamate was added to the wild type enzyme as a positive control (lane 4) while ATP alone was the negative control (lane 3). The amount of ^{32}Pi was determined by autoradiography, quantitated using densitometry, and expressed relative to the wild type enzyme without added glutamate as 100% (lane 1). The relative values are indicated below each lane. Samples are as follows: lane 1, wild type enzyme + ATP + dihydropteroate; lane 2, mutant enzyme + ATP + dihydropteroate; lane 3, buffer + ATP; lane 4, wild type enzyme + ATP + dihydropteroate + glutamate.

Assay for formation of acyl-phosphate intermediate. The first step in the FPGS reaction mechanism is the phosphorylation of enzyme-bound tetrahydrofolate or dihydropteroate by ATP to generate an acyl-phosphate intermediate [21]. This intermediate is more labile to hydrolysis than ATP. We used a TLC assay to detect the release of radioactive Pi from [γ-^{32}P]ATP by the wild type and mutant *E. coli* FPGS enzymes. After incubation with the substrates, the enzymes were boiled for 5 min to hydrolyze the acyl-phosphate intermediate. As a positive control, glutamate was added to the wild type enzyme assay mixture to allow turnover of the FPGS activity (Fig. 7, lane 4). A negative control in which glutamate was added to the assay mixture with the mutant enzyme showed only background levels of phosphate release (not shown). Assays done with either wild type or mutant enzyme in the absence of dihydropteroate had the same amount of phosphate release as the buffer control in lane 3 (not shown). The wild type enzyme showed measurable phosphate released above background levels (lane 1). The mutant enzyme had 5-fold lower level of phosphate release after subtracting background (lane 2) than the wild type, a value similar to the background level (lane 3). The E146Q mutant enzyme is therefore deficient in forming the folyl-phosphate intermediate of the FPGS reaction.

Discussion

The following is the model we postulate for the function of Glu143: This residue is required for FPGS to coordinate the Mg^{2+} and stabilize the γ-phosphate of

ATP so that the γ-phosphate can be presented to tetrahydrofolate and ATP is hydrolyzed productively to form an acyl-phosphate intermediate. When this glutamate residue is mutated, Mg^{2+} no longer binds at the functional position so that the γ-phosphate of ATP becomes flexible and binds poorly. Even an aspartate at the same position does not restore Mg^{2+} binding. The mutant enzyme is unable to form the acyl-phosphate intermediate but instead catalyzes non-productive ATP hydrolysis. Therefore, we see increased ATPase activity and defective intermediate formation in the glutamate mutant protein.

The kinetic mechanism proposed for both the *L. casei* and *E. coli* FPGS is an ordered Ter Ter mechanism with ATP as the first substrate to bind, followed by tetrahydrofolate (or dihydropteroate) and then glutamate [6,19,20]. In an ordered mechanism one would not expect the second substrate to bind to the free enzyme. However, the fluorescence studies with the wild type *E. coli* FPGS showed that dihydropteroate binds to the free enzyme with the same affinity as the enzyme–ATP complex. However, it is possible that this binding is not productive for the enzyme reaction.

Recently we solved the structure of a ternary complex of *L. casei* FPGS with ACP4-phosphate and 5,10-methylene-tetrahydrofolate [11]. There was a significant difference between the ternary complex and the binary enzyme–AMPPCP complex, resulting in a rotation of the loop linking the N-terminal domain with the C-terminal domain so that the two domains come closer together. This close conformation is more like the conformation of the corresponding domains of MurD about the active site. The nucleotide is much more firmly bound in the ternary complex with 5,10-methylene-tetrahydrofolate than in the binary complex so that the adenine ring and ribose are ordered and bound in locations identical to those of the nucleotide in the ADP-bound complex in MurD [9]. The presence of this ordered structure suggests that the nucleotide is productively bound to the enzyme in the ternary complex but was only non-productively bound in the binary complex. Thus the structural data with the *L. casei* enzyme predict that folate binding activates the enzyme for productive ATP binding. We propose that the activation that we see upon dihydropteroate or tetrahydrofolate binding to the *E. coli* FPGS is due to the same conformational change that was observed upon 5,10-methylene-dtetrahydrofolate binding in the *L. casei* ternary complex. Furthermore the conformational change observed upon 5,10-methylene-tetrahydrofolate binding is necessary to bring together the residues which are known to be required for glutamate binding and catalytic competence [11,22]. Our equilibrium dialysis studies show that the E146Q mutant is activated for ADP binding by dihydropteroate to a similar extent as the wild type enzyme. This suggests that the mutant protein is capable of undergoing the same conformational change as the wild type enzyme. Since the mutant is unable to form the acyl-phosphate intermediate, this suggests that the conformational change does not require productive ATP hydrolysis and intermediate formation.

Pteroic acid in its oxidized form, which is not a substrate for FPGS, has been previously reported to activate FPGS from beef liver [23]. In this study, pteroate had an effect only when the pteridine substrate was non-saturating and it caused a decrease in the K_m for pteridine. It was proposed that this effect was due to a conformational change. The effect of pteroate on ATP binding was not tested in their study, while we used only pteridines that were substrates of FPGS for our studies so it is difficult to tell if we are observing a similar activation.

The structure of MurD reveals a number of active site residues that correspond exactly with conserved residues in FPGS particularly those involved in ATP binding. The mechanism of catalysis of MurD has been a good model for FPGS and predicted that a conformational change was necessary to bring together the two domains of FPGS for glutamate binding and catalysis [22]. Our recent crystallographic data [11] provide evidence for this conformational change and the present data provide biochemical evidence.

Acknowledgments

The authors thank John McGuire for helpful discussions and Jun Liu for reading the manuscript. The work was supported by Grant MOP42444 from the CIHR. YS is supported by a studentship from the CIHR.

References

[1] J.J. McGuire, J.K. Coward, in: R.L. Blakeley, S.J. Benkovic (Eds.), Folates and Pterins, Wiley, New York, 1984, pp. 135–190.
[2] B. Shane, Vitam. Horm. 45 (1989) 263–335.
[3] A.L. Jackman, D.R. Newell, D.I. Jodrell, G.A. Taylor, J.A.M. Bishop, L.R. Hughes, A.H. Calvert, in: H.C. Curtius, S. Ghisla, N. Blau (Eds.), Chemistry and Biology of Pteridines, de Gruyter, Berlin, 1990, pp. 1023–1026.
[4] E. Sikora, A.L. Jackman, D.R. Newell, A.H. Calvert, Biochem. Pharmacol. 37 (1988) 4074.
[5] J.-S. Kim, B. Shane, J. Biol. Chem. 269 (1994) 9714–9720.
[6] A.L. Bognar, B. Shane, Meth. Enzymol. 122 (1986) 349–359.
[7] X. Sun, A.L. Bognar, E.N. Baker, C.A. Smith, Proc. Natl. Acad. Sci. USA 95 (1998) 6647–6652.
[8] C.A. Smith, I. Rayment, Biophys. J. 70 (1996) 1590–1602.
[9] J.A. Bertrand, G. Auger, E. Fanchon, L. Martin, D. Blanot, J. van Heijenoort, O. Dideberg, EMBO J. 16 (1997) 3416–3425.
[10] J.A. Bertrand, G. Auger, L. Martin, E. Fanchon, D. Blanot, D. Le Beller, J. van Heijenoort, O. Dideberg, J. Mol. Biol. 289 (1999) 579–590.

[11] X. Sun, J.A. Cross, A.L. Bognar, E.N. Baker, C.A. Smith, J. Mol. Biol. 310 (2001) 1067–1078.
[12] H.J. Vogel, D.M. Bonner, J. Biol. Chem. 218 (1956) 97–106.
[13] W.P. Deng, J.A. Nickloff, Anal. Biochem. 200 (1992) 81–88.
[14] B. Shane, J. Biol. Chem. 255 (1980) 5655–5662.
[15] Z. Otwinowski, W. Minor, Meth. Enzymol. 276 (1997) 307–326.
[16] J. Navaza, Acta Crystalogr. A 50 (1994) 157–163.
[17] A.T. Brunger, P.D. Adams, G.M. Clore, W.L. Delano, P. Gros, R.W. Grosse-Kunstleve, J.-S. Jiang, J. Kusznewski, M. Nilges, N.S. Pannu, R.J. Read, L.M. Rice, T. Simonson, G.L. Warren, Acta Crystallogr. D 54 (1998) 905–921.
[18] R. Ferone, S. Singer, M.H. Hanlon, S. Roland, in: J.A. Blair (Ed.), Chemistry and Biology of Pteridines, de Gruyter, Berlin, 1983, pp. 585–589.
[19] A.L. Bognar, B. Shane, J. Biol. Chem. 258 (1983) 12574–12581.
[20] A. Bognar, C. Osborne, B. Shane, S. Singer, R. Ferone, J. Biol. Chem. 260 (1985) 5625–5630.
[21] R. Bannerjee, B. Shane, J.J. McGuire, J.K. Coward, Biochemistry 27 (1988) 9062–9070.
[22] Y. Sheng, X. Sun, J.A. Cross, Y. Shen, A.L. Bognar, E.N. Baker, C.A.J. Smith, Mol. Biol. 302 (2000) 427–440.
[23] P.J. Vickers, R. Di Cecco, Z.B. Pristupa, K.G. Scrimgeour, Can. J. Biochem. Cell Biol. 63 (1985) 777–779.